Measuring and Interpreting Flame Height in Wildland Fires

Albert J. Simard, Richard W. Blank, and Sharon L. Hobrla*

Abstract

Although advanced technologies are available for measuring and sampling fire intensity, their costs, limitations, or complexity often preclude general use in field experiments. The lack of quality measurements exacerbates the task of relating ecological responses directly to the fires that cause them. In this paper, a new technique for measuring flame height, describing its distribution, and relating it to fire intensity is presented. Flame pulsation in natural fuels is also examined.

Background

The classic method of quantifying fire intensity is through a relationship given by Byram:[1]

$$I = hwr \tag{1}$$

where: I = fire line intensity [Btu/(ft × s)],
h = fuel heat content (Btu/lb),
w = fuel consumed (lb/ft^2), and
r = rate of spread (ft/s).

The heat content of dead celluosic materials does not vary greatly and can be approximated with a constant without significant loss of accuracy. Simard et al.[2,3] recently described an algorithm for accurately measuring rate of spread in the field and methods for sampling within-fire variability. An inexpensive electronic timer developed by Blank and Simard[4] can be used to facilitate data acquisition. Thus, two out of three input variables are available.

Given current technology, however, it is not possible to accurately distinguish between fuel consumed within the flaming front and fuel consumed after the flame front passes. This is of interest to fire ecologists because short-duration flaming combustion primarily affects above-ground portions of plants, whereas subsequent long-duration glowing combustion impacts roots and soil organisms. The practice of using post-fire fuel consumption for w in Equation 1 combines the two, thereby yielding inflated intensity values for the fire front.

An alternative relation developed by Byram[1] and reformatted by Rothermel and Deeming[5] is often used to estimate fire line intensity. It is:

$$I = 5.67 \, L^{\,2.17} \qquad\qquad (2)$$

where I = fire line intensity [Btu/(ft × s)] and
         L = flame length (ft).

Fire intensities estimated by Equation 2 are typically 25 to 50 percent lower than those estimated by Equation 1.* Although part of the discrepancy may result from error in Equation 2, its consistently lower values suggest that much of the difference is related to the inclusion of post-frontal fuel consumption in Equation 1. Thus, the two measures of intensity appear to provide a convenient method for distinguishing between flaming and glowing combustion.

Measuring flame length in the field, however, is fraught with problems, beginning with the definition of flame length itself: "the distance between the tip of the flame and the ground (or surface of the remaining fuel) midway in the zone of active flaming."[5] Despite carefully labeled diagrams (e.g., Figure 1), the concept is commonly misunderstood, and the wrong thing is often measured. Rothermel and Deeming further point out that "because the flame tip is a very unsteady reference, your eye must average length over a reasonable time period." This, at the same time that the eye is estimating the midpoint of the flaming zone and the distance between the two fluctuating points.

An illuminating experiment conducted by Johnson[6] used 35 two-person teams to obtain 450 independent 30-second flame length observations from steadily burning fuel piles. The range of maximum flame length observations spanned factors of 3.8 and 5.7 in two fires; the range of minimum flame length observations spanned factors of 12 to 62. Although Hough and Albini[7] and Sneeuwjagt and Fransden[8] found better correlations between observed and predicted flame lengths of less than 3 feet, Ryan[9] points out that several observers are needed to obtain adequate flame length samples due to extreme variability of fires in

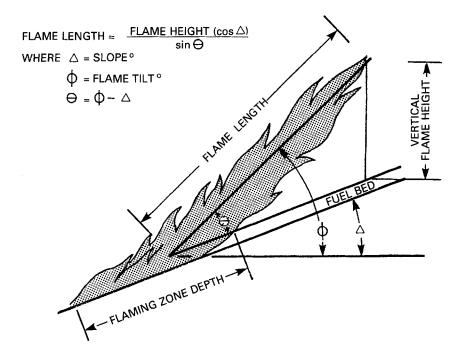*Information on file at the USDA Forest Service, North Central Forest Experiment Station, East Lansing, Michigan.

FLAME LENGTH $= \dfrac{\text{FLAME HEIGHT (cos } \triangle)}{\sin \ominus}$

WHERE $\triangle$ = SLOPE°

ϕ = FLAME TILT°

$\ominus = \phi - \triangle$

Figure 1. Flame geometry (see Ryan[9]).

slash. This, in turn, poses significant logistical and safety problems on the fire line. Ryan also notes that observer bias due to viewing angle is difficult to overcome.

Clements et al.[10] coupled triangulation algorithms with photography to measure flame geometry. Although McMahon et al.[11] used video image analysis in the laboratory and field, the professional equipment needed to capture diffuse flames is moderately expensive. The method requires that the flames be visible and "well behaved" as they approach the camera; light conditions and type of film can also affect the results. Finally, an operator must be on hand during the fire. Photography is not well suited for ignition methods other than a single line approaching the camera.

Ryan[9] developed a passive flame height sensor in which four retardant-treated strings are hung from a wire support. As a fire passes beneath the strings, they are charred to 70 percent of maximum flame height.* The height of charring is determined by running two fingers

*Ryan, K. C. USDA Forest Service, Intermountain Forest & Range Experiment Station, Missoula, Montana (personal communication).

firmly down the string until a point is reached where the fibers disintegrate. Several issues would have to be resolved prior to general use, however, including: material, degree of twisting, number of strands, size, retardant mixture, and statistical accuracy. More importantly, the procedure only supplements current methods, in that it is intended to be coupled with visual flame tilt angle observations to calculate flame length.

As with any measure of flame geometry, flame height is an ambiguous concept. Due to the ephemeral nature of wildland flames, height would be better described as a distribution of instantaneous observations. The distribution, in turn, has associated parameters such as maximum, mean, 90th percentile, etc. We must, therefore, understand how specific parameters relate to the flame height distribution. It is also important to know the relation between sampling frequency and accuracy relative to different parameters.

From another perspective, Byram and Nelson[12] found flame pulsation periods ranging from 0.2 to 1.2 seconds for liquid pool fires ranging from 0.25 to 8.0 feet in diameter. Martin et al.[13] presented thermocouple temperature data from laboratory wood crib fires that displayed large "instantaneous" fluctuations. They ascribed the fluctuations to "varying temperatures within a flame or to drawing of excess cool air from the surroundings." It is also possible that their thermocouples were reflecting the presence or absence of flame at the sample point.

Thus, in addition to describing a technique to measure flame height, we will also examine the flame height distribution, flame pulsation, and a proposed method for relating flame height to fire intensity.

Methods

After testing several alternate materials and procedures, we selected 60/40 (percent by weight) tin/lead solder. Although the tested solder includes a 3 percent (by weight) rosin core, this should have little effect on its thermal properties (solid wire solder is also readily available). The solder changes from solid to plastic at 361°F and becomes liquid at 370°F. We tested two common standard wire gages (swg):

	Nominal dimension	
swg	diameter (in.)*	area (in.²)
18	0.050	0.0020
20	0.036	0.0010

*manufacturer's tolerance: 0.002 in.

Solder is simpler to use and faster to deploy than strings under field conditions. Free-hanging solder up to 4 feet long displayed little lateral movement as experimental flame fronts passed or in gusty winds. The

solder is unaffected by rain or dew, thus allowing us to prepare a burn site well in advance of a fire.

We constructed 20 outdoor fuel beds, 4 feet long by 6 inches wide, using grass and jack pine litter. Various fuel loadings and moisture contents were used to generate flame heights ranging from 0.5 to 4.0 feet. In addition to flame height, we measured spread rate, and to the extent possible, flame zone depth. Thirteen experimental fires provided useful data; seven runs were deleted because flame heights were difficult to observe due to poor lighting or because maximum flame heights were not within the preset field of view of the camera.

A steel wire was stretched horizontally 4 feet above each fuel bed, and 10 pairs of wire solder were suspended 4 inches apart (Figure 2). Each pair consisted of one 18-gage and one 20-gage wire spaced about 1 inch apart. A painted background with 6-inch vertical marks was used to aid in observing flame height. Each fire was taped on consumer-grade video equipment from a standard photo point. The camera height was preset at the expected flame height. Although observed flame height often differed from a horizontal projection from the camera lens, we believe the measurement error to be less than 1 inch and not significant to this
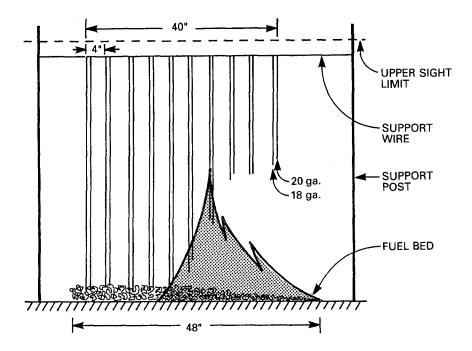

Figure 2. Flame height measurement experimental test bed. The video camera recorded the image seen in this view. Due to natural variability, the 18-gage wire occasionally melted higher than the 20-gage wire.

study. Point-specific maximum flame height measurements for each strand of solder (recorded to the nearest inch) were obtained from the videotape played back at normal speed. Height of solder melt above the ground was measured on-site (to the nearest 0.5 inch) and visually from the videotape (to the nearest inch).

We also selected three fires that spanned the flame height range (but constrained by good flame visibility) and obtained detailed flame height–time series data at three sample intervals:

1.0 second—duration of fire
0.1 second—two 10-second samples
0.017 second—two 1-second samples.

In each case, the videotape was stopped at the approximate interval and flame height was measured to the nearest inch. Flames were difficult to distinguish on individual frames due to image quality. By adjusting the playback rate, however, we established a smooth cadence so that the eye integrated flame movement and density over several frames and marked the position when the tape stopped. The minimum sample interval (average = 0.017 second) integrated three to four frames (depending on the position of the horizontal scan bar). This proved adequate for detailed flame height measurement. Consistency between separate overlapping samples indicates that flame heights were, in fact, measured to an accuracy of 1 inch.

We used regression analysis to relate the height of solder melt (H_s) to point-specific maximum flame height (H_{fm}) and to determine differences between the two solder gages. We compared differences between flame height and height of solder melt over a short distance to determine if the measurement procedure varied less, about the same, or more than the phenomena that we were measuring. A second phase of the analysis explored relations between H_s and the distribution of H_f. The purpose was to determine if a simple height measurement could yield additional descriptors of the flame height distribution.

Finally, we field tested the solder technique in three oak understory prescribed fires. We constructed 25 wire brackets 24 inches tall to hold the solder (Figure 3). By positioning the bottom bracket 1 inch above the surface, low-intensity fires were not extinguished by the bracket itself. Although two bars at right angles would eliminate possible directional bias, ease of transporting flat brackets was considered more important. We carried a spool of solder to each wire frame, and in about 1 minute, attached four strands to the top and bottom brackets. (The bottom bracket is, in fact, unnecessary for solder lengths up to 4 feet.) Unmelted solder can be reused by simply attaching a new piece between the melt point and the ground. About ten dollars' worth of solder sufficed for 25 sample points (four strands each, 2 feet high).
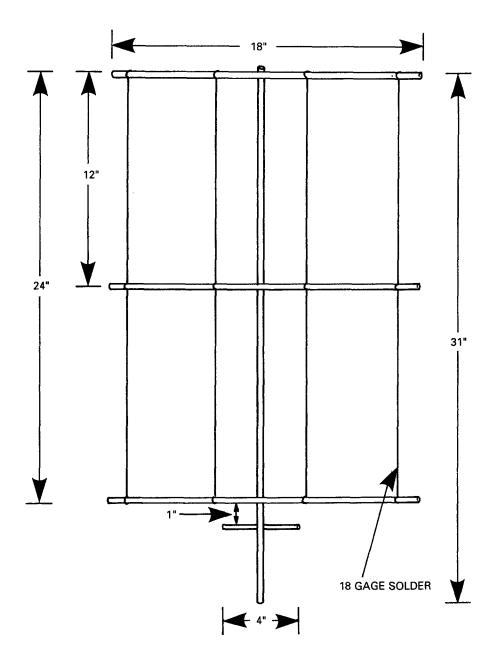
Figure 3. Wire bracket for holding solder for field application.

Results

Measuring Flame Height

Maximum point-specific flame heights (H_{fm}) for individual fires (average sample size = 17.7 points per fire) ranged from 11 to 53 inches (Table 1). The standard deviation of the maximum point-specific flame height (sH_{fm}) ranged from only 1 to 5 inches, suggesting surprising consistency for a measurement that will be shown to be highly variable on an instantaneous basis. There is no apparent relation between H_{fm} and sH_{fm} (for $H_{fm} > 10$ inches). For all 13 experimental fires, H_{fm} averaged 26 inches with an average sH_{fm} of 14 inches (Table 2). Virtually identical $\overline{H_{fm}}$ statistics for the two sets of alternating observations (18 and 20 gage) enhance data credibility, as does the 0.6-inch average difference between the camera- and ground-measured solder height data. For all fires, the height of solder melt (H_s) ranged from 5 inches to 48 inches (the upper limit of our apparatus). Average solder heights $(\overline{H_s})$ (19.6 inches for 18 gage; 21.1 inches for 20 gage) were 75 and 80 percent of $\overline{H_{fm}}$, respectively.

Three stages were observed in the solder melting process. First, there was a three- to five-second heating delay between the first contact of a flame with the wire and first melting. During the heating phase, the solder was "engulfed" by 10 to 15 flame pulses before melting began. The exact beginning of rapid melting was difficult to measure accurately

Table 1. Average flame height and rate of spread for 13 experimental fires used for flame height measurement analysis.

Fire	Maximum Flame height (in.)* (H_{fm})	(sH_{fm})	Rate of spread (ft/min) (r)
5	17.5	4.5	0.2**
6	24.4	3.5	0.4
7	17.0	4.0	0.5
8(B)	20.6	3.6	0.7
9	10.7	1.8	1.1
10	12.4	2.5	1.2
11(A)	16.8	3.2	1.0
12	36.4	2.1	1.1
13(C)	53.2	2.3	1.7
14	49.6	1.6	1.7
15	33.0	3.4	1.2
17	39.0	3.3	0.6
20	12.9	0.9	1.1

*Average sample size = 17.7.
**Spread artificially enhanced by periodic addition of dried grass.

Table 2. Flame height measurement sample statistics (n = 115).

Variable	$\overline{X}$ (in.)	s (in.)
18-gage		
Flame height (max)	26.1	14.2
Solder height (ground)	19.6	11.9
Solder height (camera)	20.1	12.8
20-gage		
Flame height (max)	26.2	14.2
Solder height (ground)	21.1	12.1
Solder height (camera)	21.7	13.2

because it was often obscured by flames. Melting did not take place continuously; rather, 3- to 6-inch lengths fell within 1 to 2 seconds after melting started. Presumably, the entire lower portion of the wire had been preheated simultaneously. In the third stage, as H_s rose above the apparently continuous flame, further melting occurred in 5 to 15 steps averaging about 1 second apart, in which 0.5 to 2.0 inches of solder melted or fell off. In the third stage, contact with one to three flame pulses preceded each melt. Final melts for individual strands were typically 0.5 to 1.0 inches long, thus defining the accuracy of the measurement technique.

Regression statistics (Table 3) indicate that H_s is an excellent predictor of H_{fm} ($R^2 = 0.96$, standard error = 2.9 inches). By using four strands at one sample point, the 95 percent confidence interval for that point is 3 inches. The scatter diagram for 18-gage solder (Figure 4) indicates that measurement errors are uniform across the full range of data. The 20-gage solder displayed a similar pattern.

Differences between 18- and 20-gage solder melt heights were not statistically significant. Results were as anticipated, however, in that the finer 20-gage wire melted an average 1.5 inches higher than the 18-gage wire due, presumably, to the former's lesser ability to absorb heat without reaching the melting temperature. An intriguing possibility is that of relating different melting heights to mass difference coupled with the solder's heat capacity to directly measure the energy output of the flame.

Table 3. Regression statistics $H_{fm} = b_0 + b_1 (H_s)$.

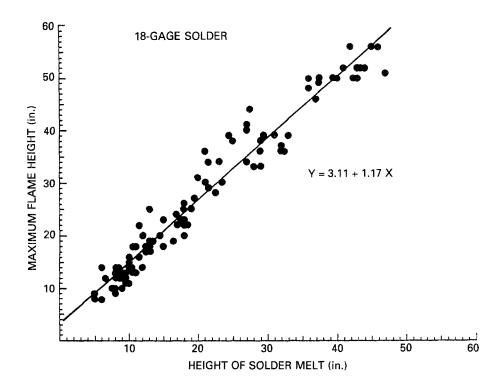| Gage	b_0	b_1	R^2	SE	SE (b_0)	SE (b_1)
18	3.11	1.17	0.96	2.95	0.53	0.023
20	1.98	1.15	0.96	2.89	0.54	0.022

Figure 4. Scatter diagram of solder height (H_s) and maximum flame height (H_{fm}) for 18-gage solder.

We found a trend of H_{fm} values within the 4-foot experimental runs. For the first two pairs of wire, H_{fm} averaged 23.8 inches for all fires, that for the last pair averaged 30.2 inches, whereas the middle 14 pairs averaged 26.4 inches with no observable trend. We surmised that both endpoint H_{fm} measurements incorporated nonsteady-state elements and, therefore, only used the middle 14 pairs for all subsequent analyses.

Average H_{fm} differences among pairs of points are shown as a function of the distance between pairs (Figure 5). Average differences between pairs of points increase to 3 inches at 14 inches apart. At greater distances, H_{fm} variability appears more random than ordered. Thus, the 95 percent confidence limit of 3 inches for measurement accuracy appears well suited to measuring flame height. Differences among H_s measurements were also plotted as a function of distance between pairs of points in Figure 5. The H_s trend approximately parallels the H_{fm} trend up to 16 inches. Between 16 and 24 inches, H_s differences appear greater than those for H_{fm}, but the former's trend is more consistent. The trend for H_s differences versus distance between points observed in three field tests also parallels that observed in our 13 experimental fires (Figure 5).
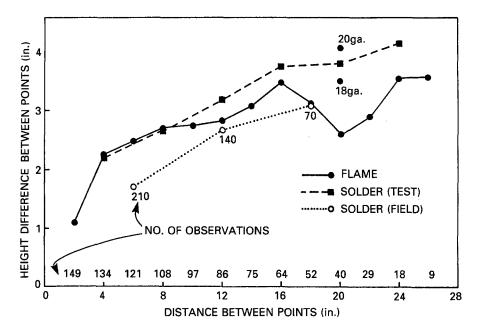
Figure 5. Average differences between maximum flame height (H_{fm}) and solder height (H_s) measurements as a function of the distance between paired points.
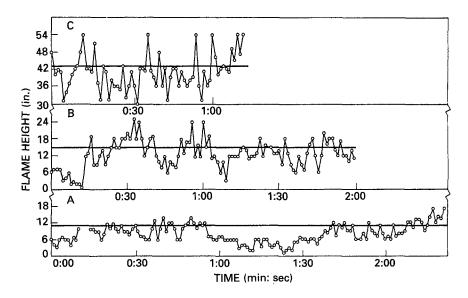

Figure 6. Instantaneous flame height (H_f) for three fires sampled at 1.0-second intervals over the middle 28 inches of a 48-inch run. (Fire A was obscured for 3 seconds at the 10-second mark.) The bold horizontal line for each fire indicates average solder height ($\overline{H_s}$).

The consistent H_{fm} and H_s trends over distance suggest that flame height variability, not measurement variability, is the prime contributor to the measurement error observed in this study.

Flame Height Distribution

A plot of instantaneous flame heights (H_f) at 1-second intervals for the middle 28 inches of three fires is shown in Figure 6. The average H_s value for the interval is indicated by the horizontal line. Figure 6 displays H_f over constant time intervals regardless of location, in contrast to the previous data that measured H_{fm} relative to fixed points—regardless of time. Perhaps the most striking feature of Figure 6 is the relative infrequency with which H_f is at its maximum value. As a result, under field conditions, traditional methods of measuring flame height (and by association, flame length) are deceptive. The ability of the eye to integrate images over time, coupled with aftereffects of bright images, would completely obscure the H_f valleys when observed in real time.

From a sampling perspective, both the 1.0- and 0.1-second samples yield H_f mean and variance values that are not significantly different at the 5 percent level. We, therefore, used the 1-second samples to examine the distribution of H_f and its relation to H_s. Selected distribution parameters for H_f and H_s are given in Table 4. For all three fires, $\overline{H_f}$ is centered in the flame height range. The mean, median, and modal flame heights for all three fires combined are within 1 inch of each other, indicating robustness in measures of central tendency.

Some H_s parameters warrant attention. First, the range of data for 18-gage solder is only 25 to 40 percent of the range of H_f. This suggests considerable damping of H_f variability by the solder measurements—a potentially useful attribute. The 20-gage solder follows the same trend, but is less consistent. Differences between $\overline{H_s}$ and $\overline{H_f}$ average 2.7 inches (18-gage) and 4.6 inches (20-gage). The narrow range of the differences suggests a constant relationship between $\overline{H_f}$ and $\overline{H_s}$ for each gage. Hence, although we did not test the possibility, $\overline{H_s}$ may be useful for estimating $\overline{H_f}$—an even more meaningful distribution parameter than H_{fm}.

By dividing each distribution into a continuous flame component (below H_{fmin}) and a variable flame component (above H_{fmin}) and converting the frequency data to a percent of the variability range, we were able to plot the cumulative distributions for all three fires on one scale (Figure 7a) and combine them into a single distribution (Figure 7b). We plotted $\overline{H_s}$ for each fire (Figure 7a) and measured the proportion of the total area of the cumulative H_f curve that was below $\overline{H_s}$. On average, for 18-gage solder, 96 percent of the total area under the cumulative H_f distribution was below $\overline{H_s}$. Of equal importance, the range of area below $\overline{H_s}$ (1.8 percent) for all three fires was surprisingly small (Table 4), suggesting a constant relationship.* On average, for 20-gage solder, 98 percent of

*Because the continuous flame area below H_{fmin} is included in the total area, the lower $\overline{H_s}$ position for Fire C is deceptive (Figure 7a).

Table 4. Distribution parameters for flame height and solder height.

a. Flame height (in.)

Fire	n	Max	Min	Range	Median	$\overline{H_f}$	sH_f
A	142	17	1	16	8.5	8.0	3.3
B	104	25	1	24	12.5	12.6	5.1
C	69	54*	30	24	41.5	40.8	6.1

b. 18-gage solder height (in.) ($n = 7$)

Fire	Max	Min	$\overline{H_s}$	sH_s	Percent Area**	Time†
A	14.5	8.5	11.2	2.5	97.0	17
B	18.0	11.5	15.2	2.8	95.2	24
C	46.0	40.0	43.2	2.1	96.1	22

c. 20-gage solder height (in.) ($n = 7$)

Fire	Max	Min	$\overline{H_s}$	sH_s	Percent Area**	Time†
A	17.5	7.0	12.2	3.6	97.9	9
B	21.0	14.0	17.4	2.4	97.3	20
C	48.5	44.0	45.5	1.7	98.1	18

*The upper limit of the visual field was 51 inches. A maximum height of 54 in. was assumed.
**Percent of total area under the flame height cumulative probability curve below $\overline{H_s}$.
†Percent of time that the sensor is in direct contact with the flame at $\overline{H_s}$.

the area was below $\overline{H_s}$, with a range of 0.8 percent.

Extrapolation, based on percent of time spent in direct contact with the flame for the two solder gages, suggests that a size decrease from 20 to 24 gage might yield a direct measurement of H_{fm}. At H_{fm}, time spent in direct contact with the flame approaches zero, and 24-gage wire, with only 40 percent of the cross-sectional area of 20-gage wire, would quickly heat to the melting point. This might be accompanied, however, by increased measurement variability and fragility under field conditions. Conversely, a size increase from 18 to 14 gage would increase the solder cross-section area by 2.8 times. This might increase the melting time lag by the right amount to yield a direct measurement of $\overline{H_f}$. This might also be accompanied by further damping of H_f variability.
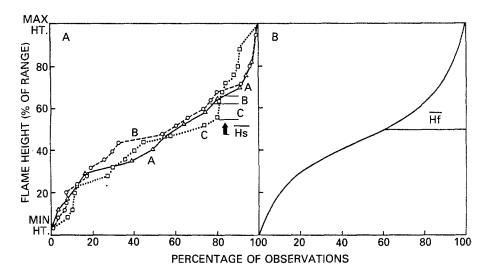
Figure 7. Cumulative frequency distribution for three experimental fires.

Flame Height and Fire Intensity

To be useful in the field, flame height should be directly relatable to fire intensity, as is the case for flame length (Equation 2). A simple relationship between flame geometry and fire intensity would assume that the advancing flame front has a triangular transverse cross-sectional area. Although an oversimplification for natural fires, it illustrates the concept and serves as a starting point. Then, by measuring flame height and flame zone depth, calculating the cross-sectional area is straightforward:

$$A_f = 0.5 \times H_f \times D_f \qquad\qquad (3)$$

where: A_f = cross-sectional area of the flaming front,
         H_f = flame height, and
         D_f = flame zone depth (front-to-back distance).

For slopes (Figure 1), H_f would be multiplied by cos Δ, where Δ = slope angle. The cross-sectional area does not depend on flame tilt angle, thus alleviating the need to visually observe that problematic variable.

We hypothesize that the cross-sectional area of a flame is at least as well related to fire intensity as flame length. It stands to reason that capturing two dimensions of the flame's geometry should, in fact, be superior to capturing just one. Further, this and previous work demon-

strate that, unlike flame length, flame height and rate of spread are measurable in the field with good accuracy. Although visual methods are still required to measure D_f, it fluctuates much less than flame length and should, therefore, be easier to observe in the field. Alternatively, flame zone depth could be measured by coupling existing electronic rate-of-spread timers with a temperature-sensitive flaming duration timer that turns on when flaming begins and turns off when continuous flaming stops. A third approach employs an approximation based on the simple relationship:

$$D_f = r \times t \tag{4}$$

where r is the rate of spread, and t is the duration of flaming combustion. If we assume that the variance of t is small, as it would be for uniform surface fuels (excluding random heavy fuel concentrations) we have $D_f \propto r$ with t a constant of proportionality. This leads to a simple approximation for fire intensity:

$$I = b_0 + b_1 (H_f \times r) \tag{5}$$

Using video image analysis and laboratory wind tunnel experiments, Nelson[14] measured the inputs to Equation 1 and flame geometry. After calculating traditional values for I, he used regression analysis to relate them to H_f and r:*

$$I = 47 + 15444 (H_f \times r); \qquad R^2 = 0.89 \tag{6}$$

where: I = fire intensity (kW/m),
          H_f = flame height (m), and
          r = rate of spread (m/s).

The relatively high R^2 partially reflects the fact that r is involved on both sides of Equation 6. It also suggests, however, that there may be a relatively simple relationship between H_f and $h \times w$ that is adequate for many purposes. If this were to hold beyond the limited sample, it would provide a method for directly evaluating Byram's intensity (I), requiring only flame height and rate of spread—two parameters that are now easily and accurately measurable. Thus, bias due to inclusion of post-frontal fuel consumption is avoided by using the proposed procedure. The key to the usefulness of Equation 6 is the variance of t (Equation 4). If the variance is small over a reasonable range of fire behavior, then the approximation could provide a useful supplement to existing methods for measuring fire intensity.

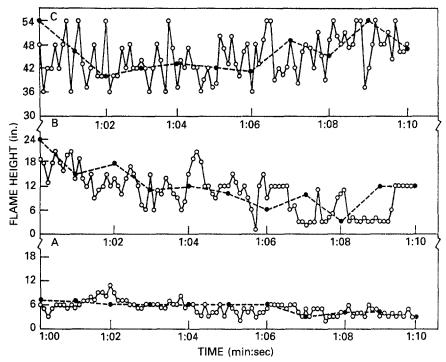*Nelson, R. M. Intermountain Forest Fire Laboratory, Missoula, Montana (personal communication).

Figure 8. Instantaneous flame height (H_f) for three fires sampled at 0.1-second intervals over a 10-second period (circles, solid lines). Solid dots and dashed lines are 1-second data for the same period.
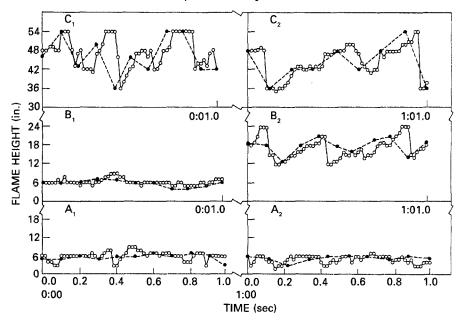

Figure 9. Instantaneous flame height (H_f) for three fires sampled at 0.017-second intervals over two 1-second periods, starting at 0:00.0 and 1:00.0 (circles, solid lines). Solid dots and dashed lines are 0.1-second data for the same period.

Flame Pulsation

Although acceptable for determining the mean and variance of H_f, the 1.0-second sample interval misses the flame's pulsation frequency and pattern. For example, compare the superimposed 1.0-second samples (solid dots and dashed lines) with the 0.1-second samples in Figure 8. At a 0.017-second interval, the true H_f frequency, amplitude, and pattern can be seen, as evidenced by sequential samples with little or no change in flame height (Figure 9). The pulsation appears as a gradual increase and a precipitous decrease. Actually, the sudden decrease often represents a flame tip that breaks away from the main flame body and is, therefore, no longer included by our sampling rules.

The 0.1-second interval does not accurately reflect the true H_f pattern, the pulsation frequency, or its amplitude (Figure 9). Although part of the mismatch is likely due to time measurement error, much of the gap between the dashed and dotted lines probably reflects the inadequacy of the 0.1-second interval. The 0.1-second samples captured 77 percent of the pulses; missed peaks averaged about half the amplitude and duration of those that were captured. For about half of the observed pulses, the 0.1-second sample accurately reflected the true maxima or minima; for the remainder, errors ranged up to 5 inches. The average error for all points is 1 inch, yielding an average amplitude error of 2 inches. (When there was a discrepancy, the 0.017-second samples invariably had higher maxima and lower minima than the 0.1-second samples.) If more than the mean and variance of H_f is needed, a 0.1-second interval appears too coarse, while a 0.017-second interval seems more detailed than necessary. A compromise of 0.05 seconds would appear to adequately reflect the true H_f pattern. At this interval, sampling error is reduced to the limits of measurement accuracy (1 inch).

Our data permit a qualitative discussion of flame pulsation in natural fuels. Fire A and Sample B1 might be best characterized as laminar and nonpulsing. In a study of pulsating liquid-pool fires, Byram and Nelson[12] noted that small-diameter fires (less than 0.5 feet in diameter) "appeared to have notable laminar features." In our tests, the fuel bed width for all fires was 6 inches and flame zone depth for A and B1 did not exceed 6 inches. Thus, the "effective diameter" of these samples seems comparable to that referred to by Byram and Nelson. In sharp contrast, B2 disclosed four pulses (defined as one peak and trough that differed by three inches or more) per second for an average period of 0.25 seconds. Flame zone depth for this sample was 16 inches. Although Byram and Nelson suggest that "most pulsations are likely to appear over burning areas that are circular or nearly circular in shape," our limited data suggest that the process can occur at length-to-width ratios as high as 4:1.

Although we do not know the "effective diameter" of a 6 × 16 inch fire, data presented by Byram and Nelson yield an approximate relation between pulsation period (t in seconds) and fire diameter (D in feet) for

liquid pool fires:

$$D = (t / 0.38)^2. \tag{7}$$

This yields an effective diameter of 0.16 feet for sample B2—smaller than either observed dimension.

The second half of the 0.1-second sample for Fire B displays characteristics common to both B1 and B2—that is, apparent laminar and turbulent behavior (Figure 8). Byram and Nelson noted that 1- and 2-foot diameter liquid fuel fires "were probably in the transition region between laminar and turbulent flow." Although our effective diameter for Fire B differs from theirs, our data also suggest a transition region for fires in natural fuels.

Fire C was clearly pulsating (C1 = 0.17 seconds per pulse; C2 = 0.33 seconds per pulse). Although flame zone depth could not be measured, that for C1 must have been close to 14 inches and that for C2 must have been in the range of 22 to 42 inches. Thus, for Fire C, an increased pulsation period appears associated with increased flame zone depth, as predicted by the liquid pool fires. Although these results are only suggestive, they imply that flame pulsation in liquid pool fires appears poorly related to that in natural fuels in a quantitative sense, but well related qualitatively.

Summary

This paper describes a new method for measuring and interpreting flame height. Measurement involves hanging solder wires from a metal frame. The technique was tested on 13 test bed fires with flame heights ranging from 0.5 to 4 feet and on three prescribed burns. The solder melted in three phases: preheating, rapid melting, and final melting. The last phase took place in steps of 1 inch or less, delineating the accuracy limit of the technique. Maximum flame heights varied by about 3 inches over an 18-inch distance, delineating the inherent small-scale variability of the phenomenon, and hence the lower accuracy limit of meaningful information.

Melt heights of 18- and 20-gage solder were compared with measured flame height parameters. For 18-gage solder, melt height averaged 75 percent of the maximum flame height and 2.7 inches above the average flame height. Regression analysis indicated that four strands, 6 inches apart, yield a measurement accuracy of 3 inches, 95 percent of the time. The solder also integrates the cumulative effect of 20 to 40 flame pulses and, hence, dampens measurement variability. We speculate that 14-gage solder would directly measure average flame height and 24-gage solder would directly measure maximum flame height.

The hanging solder technique provides a simple and inexpensive method for passively measuring and sampling flame height with un-

precedented accuracy in the field. When coupled with other techniques for accurately measuring rate of spread, and/or flame zone depth, information is available to approximate the cross-sectional area of a flame. A method for relating flame geometry to fire intensity was presented. Regression equations, using data from an independent wind tunnel study, suggest that the proposed procedure shows promise. If generally applicable, it could enhance our ability to quantify fire behavior in the field.

We observed three categories of flame pulsation: nonpulsing, transition, and pulsing. In the latter case, the pulsation period ranged from 0.17 to 0.33 seconds. The rapid pulsation rate overwhelms the eye's ability to accurately visualize flame geometry; it may also affect laboratory measurements. A sample interval of 1 second is adequate for flame height distribution parameters such as mean and standard deviation. A sample interval of 0.05 seconds is probably needed to accurately measure maximum flame height, pulsation rate, and the flame height time-series pattern.

References

[1] Byram, G.M., "Combustion of forest fuels," Davis, K.P. (Ed.) *Forest Fire Control and Use, First edition,* McGraw Hill Book Co., New York (1959).

[2] Simard, A.J., Deacon, A.G., & Adams, K.B., "Nondirectional sampling of wildland fire spread," *Fire Technology,* **18**, 221–228 (1982).

[3] Simard, A.J., Eenigenburg, J.E., Adams, K.B., Nissen, R.L., & Deacon, A.G., "A general procedure for sampling and analyzing wildland fire spread," *Forest Science,* **30**, 51–64 (1984).

[4] Blank, R.W., & Simard, A.J., "An electronic timer for measuring spread rates of wildland fires," USDA, Forest Service, North Central Forest Experiment Station, Res. Note NC–304, E. Lansing, MI (1983).

[5] Rothermel, R.C., & Deeming, J.E., "Measuring and interpreting fire behavior for correlation with fire effects," USDA, Forest Service, Intermountain Forest and Range Experiment Station, Gen. Tech. Rpt. INT-93, Ogden, UT (1980).

[6] Johnson, V.J., "The dilemma of flame length and intensity," USDA, Forest Service, *Fire Management Notes,* **43**, 3–7 (1982).

[7] Hough, W.A., & Albini, F.A., "Predicting fire behavior in Palmetto-Gallbury fuel complexes," USDA, Forest Service, Southeastern Forest Experiment Station, Res. Pap. SE–174, Asheville, NC (1978).

[8] Sneeuwjagt, R.J. & Fransden, W.H., "Behavior of experimental grass fires vs. predictions based on Rothermel's fire model," *Canadian Journal of Forest Research,* **7**, 357–367 (1977).

[9]Ryan, K.C., "Evaluation of a passive flame-height sensor to estimate forest fire intensity," USDA, Forest Service, Pacific Northwest Forest & Range Experiment Station, Res. Note PNW–390, Portland, OR (1981).

[10]Clements, H.B., Ward, D.E., & Atkins, C. W., "Measuring fire behavior with photography," *Photogrametric Engineering and Remote Sensing,* **49,** 213–217 (1983).

[11]McMahon, C.K., Adkins, C.W., & Rodgers, S.L., "A video image analysis system for measuring fire behavior," USDA, Forest Service, *Fire Management Notes,* **47,** 10–14 (1986).

[12]Byram, G.M. & Nelson, R.M., "The modeling of pulsating fires," *Fire Technology,* **6,** 102–110 (1970).

[13]Martin, R.E., Cushwa, C.T., & Miller, R.L., "Fire as a physical factor in wildland management," In *Proceedings of the ninth tall timbers fire ecology conference,* Tallahassee, FL, 271–288 (1969).

[14]Nelson, R.M., "Measurement of headfire intensity in litter fuels," In *Proceedings of prescribed burning in the Midwest: State of the art,* Stevens Point, WI, 38–44 (1986).